Original Article

PMP

Progress in Medical Physics 28(4), December 2017
https://doi.org/10.14316/pmp.2017.28.4.171
pISSN 2508-4445, eISSN 2508-4453

Simulation and Experimental Studies of Real-Time Motion Compensation Using an Articulated Robotic Manipulator System

Minsik Lee*, Min-Seok Cho*, Hoyeon Lee†, Hyekyun Chung†, Byungchul Cho*

**Department of Radiation Oncology, Asan Medical Center, University of Ulsan College of Medicine, Seoul, †Department of Nuclear and Quantum Engineering, Korea Advanced Institute of Science and Technology, Daejeon, Korea*

Received 7 December 2017
Revised 14 December 2017
Accepted 15 December 2017

Corresponding author
Byungchul Cho
(cho.byungchul@gmail.com)
Tel: 82-2-3010-4437
Fax: 82-2-3010-6950

The purpose of this study is to install a system that compensated for the respiration motion using an articulated robotic manipulator couch which enables a wide range of motions that a Stewart platform cannot provide and to evaluate the performance of various prediction algorithms including proposed algorithm. For that purpose, we built a miniature couch tracking system comprising an articulated robotic manipulator, 3D optical tracking system, a phantom that mimicked respiratory motion, and control software. We performed simulations and experiments using respiratory data of 12 patients to investigate the feasibility of the system and various prediction algorithms, namely linear extrapolation (LE) and double exponential smoothing (ES2) with averaging methods. We confirmed that prediction algorithms worked well during simulation and experiment, with the ES2-averaging algorithm showing the best results. The simulation study showed 43% average and 49% maximum improvement ratios with the ES2-averaging algorithm, and the experimental study with the QUASAR™ phantom showed 51% average and 56% maximum improvement ratios with this algorithm. Our results suggest that the articulated robotic manipulator couch system with the ES2-averaging prediction algorithm can be widely used in the field of radiation therapy, providing a highly efficient and utilizable technology that can enhance the therapeutic effect and improve safety through a noninvasive approach.

Keywords: Articulated robotic manipulator, Real-time tumor tracking, Prediction algorithm, ES2-averaging

Introduction

The main aim of radiation therapy is to kill cancer cells to the greatest extent possible while protecting normal tissues from damage. To achieve this, radiation should be precisely targeted. In recent years, more advanced techniques for radiation therapy, such as stereotactic body radiation therapy (SBRT) and image-guided radiotherapy (IGRT), require to be delivered with even greater accuracy.

There are various approaches for managing respiratory-induced motion of organs and tumors.[1] Breath-holding methods, including active breathing control (ABC) and deep-inspiration breath-holding (DIBH), are based on the patient controlling his/her own breathing with or without the assistance of appropriate devices. However, many patients with lung cancer have pulmonary function insufficiency and may, therefore, have difficulty with breathing control and experience discomfort during

treatments. Methods of adapting the beam to tumor motion while the patient breathes freely are useful for such cases. Respiratory gating is widely used in clinical treatment; this technique involves holding back the beam until the target returns within a certain gating window. However, drawbacks of this method are the prolonged treatment time and a low duty cycle, normally of <30%.[2,3] Irregular breathing or baseline shifts also reduce the accuracy of gating.[4] Unlike the breath-holding and gating techniques, real-time tumor tracking with a dynamic multi-leaf collimator (DMLC) enables a 100% duty cycle and allows the patient to breathe freely, but a limitation is the delay in leaf positioning when the direction of tumor motion has a component perpendicular to the direction of leaf motion. This DMLC tracking technique best maintains tracking performance when the tumor and leaf motions are in a similar direction.[3] However, studies have shown that lung tumors can move several centimeters in any direction during irradiation, regardless of the tumor size, location, and pulmonary function.[5]

Thus, couch-based real-time correction methods are being studied by many groups. Real-time tumor tracking via couch control involves detecting respiratory motion and dynamically repositioning the treatment couch to track the tumor's changing position. Because of difficulty in detecting the tumor itself, surrogate markers (external fiducials on the skin surface or internal fiducials directly implanted into the tumor) are used. Effective prediction algorithms predict the displacement of the marker, including compensation for the latency between the measurement and robot operation. Many prediction algorithms have been studied and published, including the Kalman filter,[6-8] artificial neutral networks,[6,9] probabilistic approaches,[10] the autoregressive moving average model,[11] the multi-step linear method,[12] and wavelet-based multiscale autoregression.[13] Most of the previous studies implemented a parallel robotic manipulator, which consists of a rigid body top plate, connected to a fixed base plate and is defined by at least three stationary points on the grounded base connected to six independent kinematic legs. It is also known as the Stewart platform, where all the actuators move simultaneously. PerfectPitch™ (Varian, USA), Protura™ Robotic Patient Positioning System (CIVCO Medical Solutions, IA), and HexaPOD™ evo RT System (Elekta, Sweden) are examples of this kind of 6-DOF couch.[14] However, the Stewart platform couch itself has physical limits on its motion, corresponding to 3~4 cm in each of the three physical dimensions; once a limit is reached, the couch simply cannot move any further, even though it is enough to cover the organ movement.[15,16]

In this study, therefore, we built a miniature couch tracking system comprising an articulated robotic manipulator enables a wide range of motions that a Stewart platform cannot provide. We performed simulations and experiments for investigating the feasibility of the system and proposed ES2-averaging prediction algorithms.

Materials and Methods

Main components of a treatment couch-based real-time motion compensation system are the tracking system, robot controller, and articulated robotic couch. Fig. 1 shows a schematic illustration of such a system.

1. General setup

1) An optical 3D tracking system

An optical 3D tracking system was used to simultaneously track the motions of a phantom that mimicked respiratory motion and a robotic couch. To achieve this, external markers were placed on the phantom and couch. If a passive-type infrared reflective marker was attached to an object, the tracking system could determine its relative coordinates by measuring the signal reflected from the object. We used Polaris Spectra™ (NDI Medical, Canada) as the tracking system; this is a proven device that has been tested and used with various medical devices. It has a root-mean-square accuracy of 0.25 mm and a sampling frequency of 30 Hz, and it communicates with the robot control personal computer (PC) through a USB serial port at up to 1.2 Mbps maximum transmission speed. It has a pyramidal measurement range of up to 2,400 mm (with some options offering 3,000 mm), and 6-DOF information can be extracted and saved as a log file to allow checking.

The tracking system measured the position of the markers relative to the center of the coordinate space by

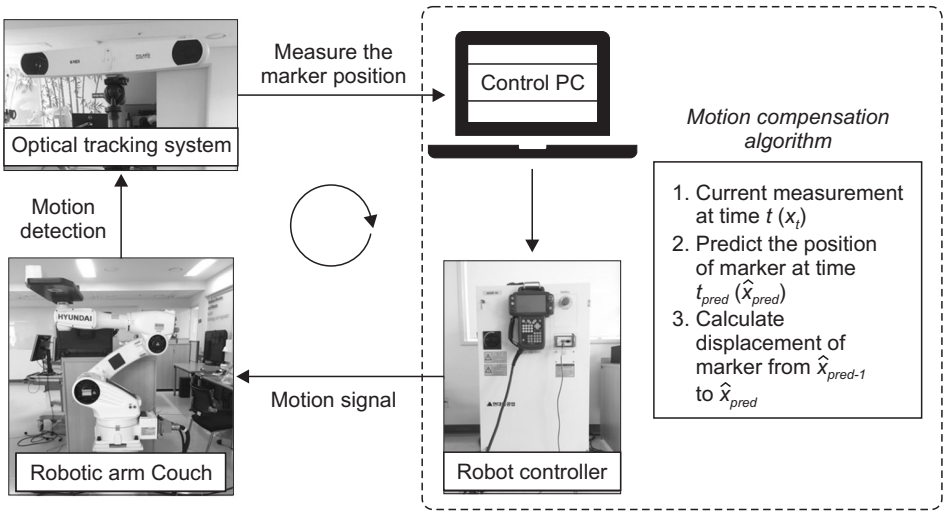

Fig. 1. Schematic illustration of a couch-based real-time motion compensation system.

measuring the spatial coordinates and rotation of each marker. The center of the coordinate space is the location of the tracking system. The rotation of the marker was represented as a quaternion; a method for describing the rotation using a rotation vector and the rotation angle. If an object is rotated at an angle θ about a unit vector ($\hat{x}$, $\hat{y}$, and $\hat{z}$), then the rotation can be described by the following quaternion:

$$q_0 = cos\left(\frac{\theta}{2}\right),\ q_x = \hat{x}\,sin\left(\frac{\theta}{2}\right),\ q_y = \hat{y}\,sin\left(\frac{\theta}{2}\right),\ q_z = \hat{z}\,sin\left(\frac{\theta}{2}\right) \quad (1)$$

Quaternions are less intuitive than Euler angles, but they avoid the gimbal lock problem that arises with Euler angles. This method is, therefore, widely used in the field of robotics as a representation of rotation.[17]

The output, saved as a text file, had a total of seven parameters: three spatial coordinates and four for the quaterion. These defined the position and rotation of the marker, which could then be used by motion detection and control software.

2) Robotic couch and controller

A six-axis articulated robotic manipulator (HA006-04, Hyundai Heavy Industries Co., Ltd., Korea), optical 3D tracking system, and robot controller were connected to PC and controlled as an integrated system. The treatment couch, made of carbon fiber, was connected to the last link of the articulated robotic manipulator. The weight capacity of the industrial six-axis vertical articulated robot was 6 kg. The couch system was capable of translational as well as rotational motion. Mechanical parameters and specifications were summarized in our previous study.[2]

To control the robotic couch, we modified the software for measuring the signal using the tracking system so that it sent the couch a displacement signal. The software used the same framework as the tracking system to measure the position of the marker. We modified the software to measure and predict the position of the marker and send an appropriate compensation signal to the robotic couch.

To determine the displacement signal to be sent to the couch, the tracking system first measured the position of the marker and then used this to calculate its predicted position; the displacement signal for the predicted position was then sent to the robotic couch for the compensation. A simplified description of the motion compensation algorithm is presented as the dashed-line rectangle in Fig. 1.

Because the tracking system measured the marker position, coordinates needed to be calibrated with those of the couch. For this calibration, coordinates were measured at seven different positions: the center and at 10 cm from the center in each of the superior–inferior, medial–lateral, and anterior–posterior directions. This resulted in seven measured coordinates and seven actual coordinates of the marker (N=7). We used singular value decomposition to establish the rotation matrix. For the measured coordinates set $\{m_i\}$ and real coordinates set $\{r_i\}$, we minimized the least-square error (E) between them through a rotation (R) and translation (T) matrix as follows:

$$E = \sum_{i=1}^{N} \left\| m_i - Rr_i - T \right\|^2 \quad (2)$$

We first removed the translational dependency by subtracting the centroid of each set to calculate R. The centroid of each set was calculated as in Eq. 3 and subtracted from each coordinate according to Eq. 4:

$$m_c = \frac{1}{N} \sum_{i=1}^{N} m_i \, , r_c = \frac{1}{N} \sum_{i=1}^{N} r_i \quad (3)$$

$$r_i^c \equiv r_i - r_c \, , \; m_i^c \equiv m_i - m_c \quad (4)$$

The error then only depended on the rotation matrix (R). The rotation matrix minimized error can be calculated by matrix multiplication (*) of the lower and upper matrices of the singular value decomposition (SVD) result of H in Eq. (5)

$$H = \sum_{i=1}^{N} m_i^c * \left(r_i^c \right)^T \quad (5)$$

After calculating the rotation matrix, we calculated the translation matrix by applying the rotation matrix to the centroid of measured and real coordinates as follows:

$$T = m_c - R * r_c \quad (6)$$

The calibration was performed immediately before sending the predicted displacement signal to the robotic couch.

2. Prediction algorithm

For the couch control to compensate for breathing-induced motion, we used the method of predicting the next position of the phantom. When patient motion data detected by the tracking system was sent to the robot controller as an input signal, there was a delay time between the measurement and robot operation, which depended on the work environment or specification. It was, therefore, necessary to measure the latency for making appropriate predictions for a given environment. Some related studies have proposed the main qualitative criteria for choosing the prediction algorithm.[18] A prediction algorithm needs to allow fast calibration for each new patient and should be able to reflect, in real time, the movement of the tumor with the patient's respiration. In addition, the method should preferably be easy to implement with any hardware system. In this study, we applied linear extrapolation (LE) and a slightly modified double exponential smoothing (ES2) algorithm.

1) Linear extrapolation

Linear extrapolation (LE) is a prediction method based on the most recent measurement values. No calibration or conditions are required, and the calculation is simple, allowing it to be easily applied to any hardware or equipment. If the current time is t and the time the prediction is required for is $t+h$, then it is assumed that the signals from $t-h$ to t are of the same size and in the same direction. This can be expressed as follows:

$$\hat{x}_{t+h} = x_t + (x_t - x_{t-h}) \quad (7)$$

2) Double exponential smoothing

Exponential smoothing is a type of moving average, where the importance of past observations decreases exponentially.[2] The double exponential smoothing (ES2) method needs no patient-specific calibration and can predict the position at the desired time immediately when motion is detected. It reflects the tumor motion and is easy to implement. This method operates well when there are trends in data. ES2 computes an evolving trend equation using a special weighting function that places the greatest emphasis on the most recent time. Instead of a global trend equation, this technique uses a local trend equation. It calculates α to measure the level which can be called the y-intercept of the trend and it also incorporates β to create a linear trend for the prediction. The ES2 algorithm can be expressed as follows:

$$\begin{aligned} \hat{x}_{t+h} &= s_t + hb_t \\ s_t &= \alpha x_t + (1 - \alpha)(s_{t-1} + b_{t-1}) \\ b_t &= \beta (s_t - s_{t-1}) + (1 - \beta) b_{t-1} \end{aligned} \quad (8)$$

where α is the level smoothing factor and β is the trend smoothing factor, which are both between zero and one; in this study, α=0.7 and β=0.6 were used. The parameter s_t

gives the y-intercept (level), whereas b_t is the slope at time t. The both smoothing factors determine how fast the weights of the series forgets. A smoothing factor near one puts almost all weight on the most recent observations, whereas a smoothing factor near zero allows the past observations to have a greater effect. ES2 requires initialization because the prediction for time 1 requires the data value for time 0, which would not be available. Thus, $s_0=x_0$ and $b_0=0$ were used as initial values. A structural limitation of this method is that a change in direction in the signal from positive to negative or vice versa results in excessive prediction.

In this study, we used a slight variation of the ES2 model to include noise reduction by applying the average filter before the prediction. Because the phantom and couch motions constantly affect each other, even a small amount of noise or jitter tends to be amplified, depending on the patient conditions. Fig. 2 schematically shows the method of applying a filter to the results prior to the prediction (ES2-averaging). The prediction algorithm starts with the measured position of the marker on the phantom relative to that of the marker on the couch at times t and t–1. The dashed lines indicate the averaging process. The new averaged position at t ($\hat{x}_t$) was obtained by averaging the measured positions at times t and t–1 and the position predicted for time t+1 by the ES2 algorithm at t. This value was then used as the input to the ES2 algorithm to predict the final value $\hat{x}_{pred}$.

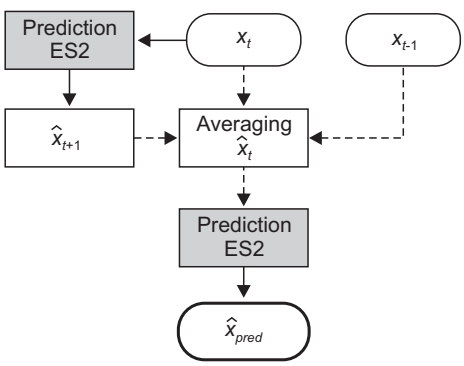

Fig. 2. Double exponential smoothing algorithm with the averaging method (ES2-averaging).

3) Test phantom

To ensure that the robotic couch appropriately compensated for the movement of the phantom by following that motion, we tested prediction algorithms described above with a stage rotation phantom (Varian, USA) which moved in a regular cycle, allowing the latency to be measured, and a QUASAR™ respiratory motion phantom (Modus QA, Canada), which could import and mimic patient breathing data.

The stage rotation phantom performed sinusoidal motion that rotated a flat circular shape plate at a constant speed and amplitude. We used this phantom separate from the couch to measure the latency. The QUASAR™ phantom could be operated so that it followed actual patient breathing motion loaded via a PC. Patient motion data were acquired from 12 patients using the Varian RPM system (Varian, USA) during four-dimensional computed tomography simulation over 300 s. We assumed that the movement of a marker placed on the objects accurately represented the movement of the tumor. The experiments were performed by attaching a marker to the couch and

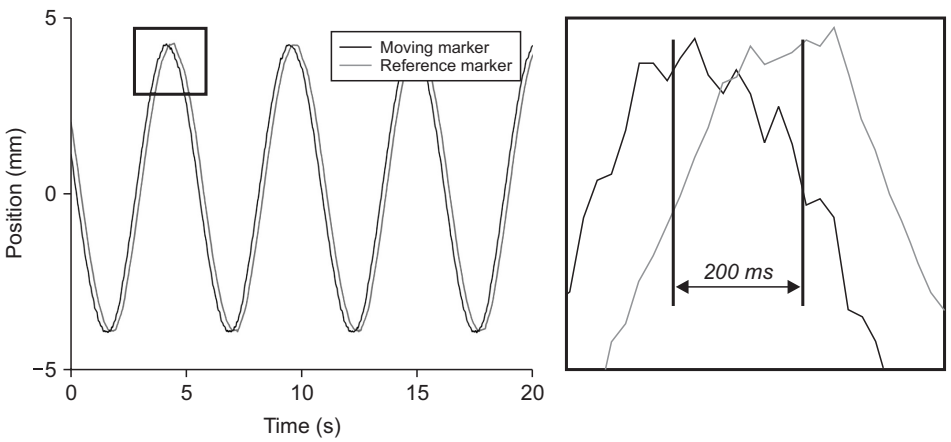

Fig. 3. Marker displacement on the rotation phantom and couch, obtained using the tracking system without applying a prediction algorithm. The inset shows a segment of the same signal.

another to the phantom.

Results and Discussion

1. Analysis of couch dynamics (latency)

The experiment using the stage rotation phantom showed the average latency between the measurement and robot operation to be 200 ms. Fig. 3 shows the marker displacement data acquired by the tracking system without applying a prediction algorithm. This shows that the movement of the couch followed that of the phantom with an interval corresponding to the latency.

2. Patient respiratory motion

We firstly performed simulations based on the patient respiratory data to ensure that prediction algorithms performed how accurately in the absence of external influences. Without the prediction algorithms, the average root-mean-square error (RMSE) value for the 12 patients was 1.96±0.29 mm, whereas using the LE algorithm it was 1.29±0.23 mm. And with the simple ES2 and ES2-averaging algorithms were 1.23±0.20 and 1.10±0.17 mm, respectively.

Table 1. Three-dimensional RMSE values and improvement ratios in the simulation study

Patient number	3D RMSE (mm)				Improvement ratio (%)		
	No Prediction	LE	ES2	ES2 (averaging)	LE	ES2	ES2 (averaging)
1	2.22	1.56	1.48	1.34	29.77	33.24	39.86
2	2.21	1.58	1.51	1.35	28.23	31.47	39.07
3	1.81	1.18	1.13	1.02	34.89	37.57	43.71
4	1.83	1.19	1.13	1.05	35.03	38.52	42.86
5	1.34	0.85	0.81	0.73	36.96	39.72	45.71
6	1.82	1.20	1.17	1.03	34.29	35.86	43.67
7	2.42	1.54	1.42	1.24	36.23	41.34	48.87
8	1.90	1.14	1.10	1.01	40.19	42.15	47.04
9	2.04	1.39	1.33	1.20	31.92	34.95	40.98
10	1.70	1.15	1.09	0.98	32.46	35.81	42.32
11	2.19	1.54	1.41	1.21	29.62	35.89	44.81
12	1.97	1.22	1.18	1.08	38.00	40.02	45.18
Mean±SD	1.96±0.29	1.29±0.23	1.23±0.20	1.10±0.17	33.97±3.66	37.21±3.26	43.67±2.88

Table 2. Three-dimensional RMSE values and improvement ratios for the experimental study using the QUASAR™ phantom

Patient number	3D RMSE (mm)				Improvement ratio (%)		
	No Prediction	LE	ES2	ES2 (averaging)	LE	ES2	ES2 (averaging)
1	2.78	2.33	1.79	1.55	16.19	35.61	44.09
2	2.76	2.43	2.09	1.57	11.96	24.28	43.27
3	2.26	1.83	1.43	1.02	19.03	36.73	54.99
4	2.29	1.87	1.33	1.06	18.34	41.92	53.58
5	1.68	1.17	1.03	0.91	30.36	38.69	45.58
6	2.28	1.82	1.68	1.05	20.18	26.32	53.88
7	3.02	2.69	1.68	1.37	10.93	44.37	54.59
8	2.38	1.78	1.36	1.30	25.21	42.86	45.29
9	2.55	2.26	1.62	1.20	11.37	36.47	52.94
10	2.13	1.78	1.27	0.96	16.43	40.38	54.93
11	2.74	2.44	1.64	1.20	10.95	40.15	56.20
12	2.46	1.89	1.36	1.12	23.17	44.72	54.47
Mean±SD	2.44±0.36	2.02±0.42	1.52±0.28	1.19±0.22	17.84±6.20	37.71±6.53	51.15±4.97

The LE algorithm showed a 34% average improvement in RMSE and a 40% maximum improvement compared with the results without a prediction algorithm. The simple ES2 algorithm showed 37% average and 42% maximum improvements, and the ES2-averaging algorithm showed 44% average and 49% maximum improvements. The ES2-averaging method showed the best results out of the prediction algorithms in the simulation study. In the experimental tests using the QUASAR^{TM} phantom with patient breathing data, the mean RMSE value of the 12 patients without applying any prediction algorithm was 2.44±0.36 mm, whereas that with the LE algorithm was 2.02±0.42 mm. And that with the simple ES2 and ES2-averaging algorithms were 1.52±0.28 and 1.19±0.22 mm, respectively. The LE algorithm showed an 18% average and a 30% maximum improvement in RMSE compared with the results using no prediction algorithm. The simple ES2 algorithm showed 38% average and 45% maximum improvements and the ES2-averaging algorithm showed 51% average and 56% maximum improvements. The detailed simulation and experimental results are presented in Tables 1 and 2, respectively.

RMSE values have meaning when obtained under the same conditions to compare the absolute accuracy, but comparing values acquired from different conditions is meaningless. In other words, absolute RMSE values of the simulation and experiments need not be considered, but improvement ratios calculated for each of the prediction algorithms (i.e., the ratio of the mean RMSE value for the algorithm to the mean RMSE value when no algorithm was applied) are of significance. Fig. 4 shows improvement ratios for the simulation and the experimental studies. In all simulation cases, the ES2-averaging algorithm was the best; on an average, 6% better than the simple ES2 and 10% better than the LE algorithm. Similarly, the ES2-averaging was also the best in all experimental cases; on an average, 13% better than the simple ES2 and 33% better than the LE algorithm.

Among the three prediction algorithms that we compared, it may be intuitively expected that ES2 would perform better than LE. The LE algorithm can predict relatively accurate results with a regular signal, but it is difficult to guarantee reasonable results with irregular signals, such as patient respiratory motion, because the LE algorithm is based on the assumption that the signal will maintain the same velocity and direction as last observed. Conversely, the ES2 method is used when there is a trend in the signal and it provides a more reasonable prediction by calculating the two parameters; the level and slope of the predicted value. In addition, the analysis of the ES2-averaging algorithm is also important. We tried to reduce the amplified noise or jitter by using the averaging filter. ES2-averaging outperformed simply ES2; we consider this to be because the ES2-averaging algorithm can reduce random errors in original data by averaging the three values before the prediction. Because the final prediction value has been predicted in that state, it can be regarded as having only prediction errors. Conversely, in simple ES2

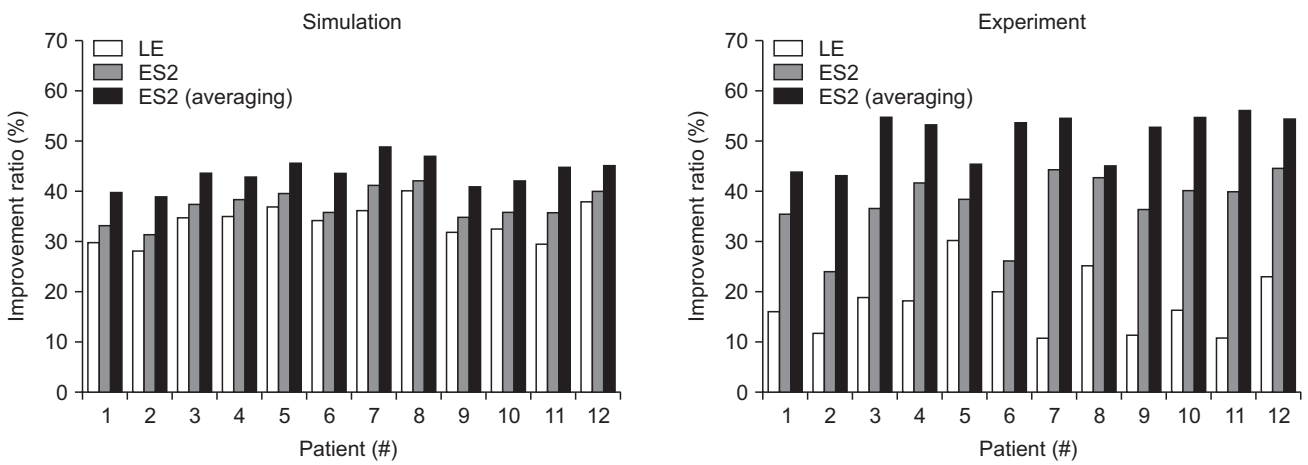

Fig. 4. Improvement ratios for the simulation and experimental studies.

methods, random errors in original data still present and the errors of the algorithm itself also remain intact.

During the qualitative evaluation, the couch moved in the opposite direction to the phantom motion to compensate for its movement motion; the ideal result would, therefore, be one showing no relative motion between the phantom and couch. Fig. 5 shows marker displacements for one (patient 5) out of 12 patients studied with the various prediction algorithms in the experimental study. Only 60 s of total breathing is displayed. As can be observed from the phantom movements (indicated by the thick line), results for the ES2-averaging algorithm approached the closest to zero relative movement; this exhibited the smallest amplitude, although there existed noise at the plateau region with every patient.

A point to consider is the reason why the improvement ratio differed between patients for the same prediction method. Comparing the cases with the best and the worst improvement ratios shows that the respiratory cycles of the patients differed. The best patient case took approximately nine and half breaths over a 60 s period, whereas the worst case took approximately 14 breaths in the same time. As described earlier, one feature of the ES2 prediction algorithm is a tendency to excessively predict when the signal direction reverses. A possible explanation of the variation, therefore, is that a smaller number of changes from expiration to inspiration (a longer respiratory cycle) may result in a lower RMSE value and higher improvement ratio. Indeed, the rest of the cases showed similar results, with the patients with shorter respiratory cycles having higher RMSE values and lower improvement ratios. In addition, the reason that the improvement ratio of the

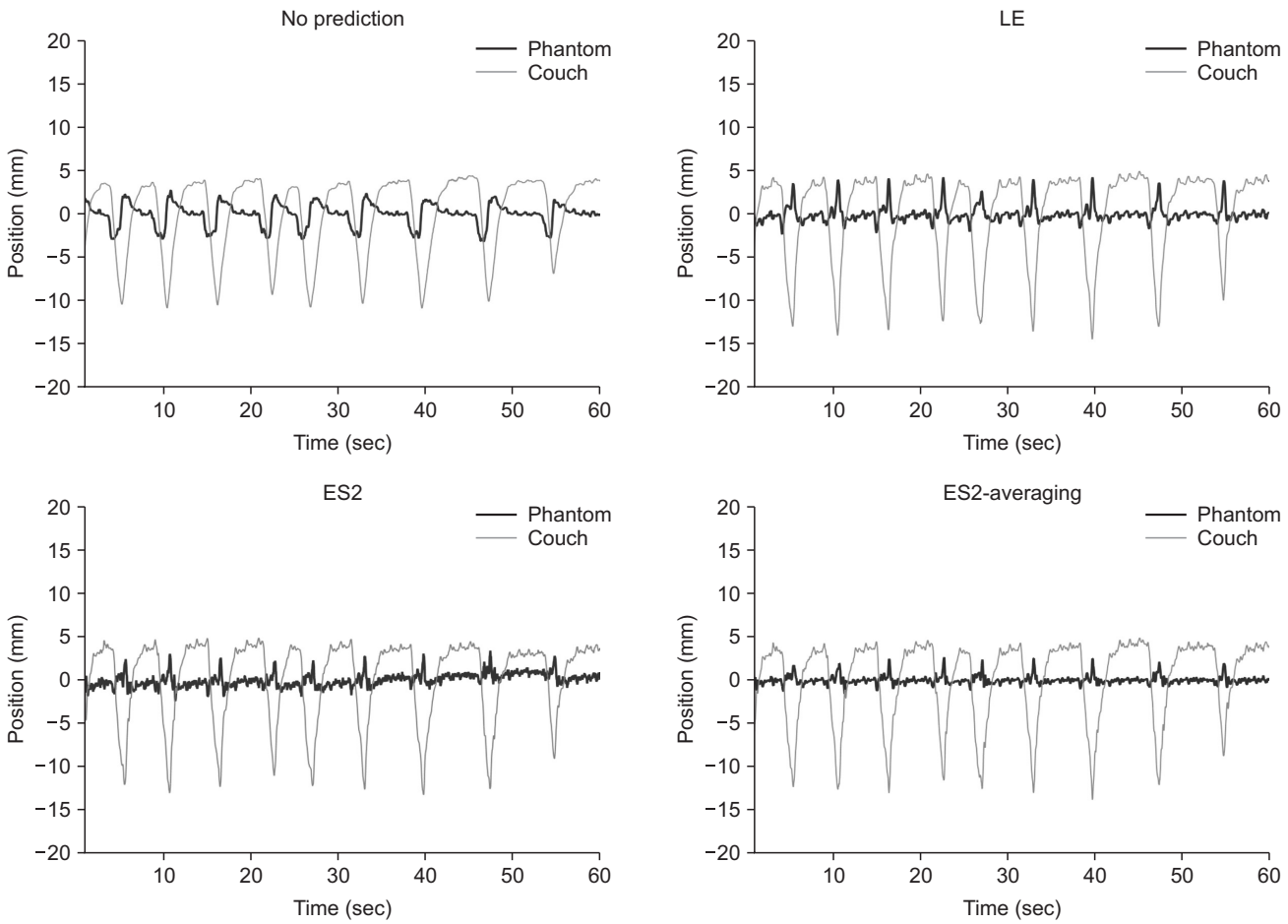

Fig. 5. Marker displacements for one (patient 5) out of 12 patients when applying the various prediction algorithms in the experimental study. The thick line indicates the phantom motion; ideally, this should appear still, indicating no relative movement between the phantom and couch.

experimental results is better than the simulation is the RMSE value of no prediction, which is the standard, is about 0.5 mm lower in the simulation on average. And it is considered that the generated noise in the experiments is reduced by the averaging effect. In the simulation without the mechanical vibration, as mentioned, the difference of improvement ratio between the ES2 and ES2-averaging is about 6%, whereas the experiment shows a noticeable difference of improvement ratio 13%.

Conclusion

The purpose of this study was to install a system that compensates for the movement of a tumor due to the patient's respiration by moving the articulated robotic manipulator couch and to evaluate the performance of the proposed prediction algorithms. We applied LE, simple ES2 and ES2-averaging algorithms which can predict the latency in advance. We confirmed that the prediction algorithms worked properly in simulation and experiments and that the ES2-averaging algorithm showed the best results.

Our results suggest that the articulated robotic manipulator couch system with the ES2-averaging prediction algorithm could be widely used in the field of radiation therapy because it is a highly efficient and utilizable technology that can enhance the therapeutic effect and improve safety through a noninvasive approach.

However, because of limitations of the current prediction algorithm, we are planning to develop a method for predicting the location of a tumor using one of the machine learning techniques for better prediction results. At the same time, we plan to test the current system in a real treatment environment and evaluate the dosimetric effects on the treatment of couch tracking.

Acknowledgements

This work was supported by the Radiation Technology R&D program (2013M2A2A7043506) through the National Research Foundation of Korea funded by the Ministry of Science, ICT & Future Planning.

Conflicts of Interest

The authors have nothing to disclose.

Availability of Data and Materials

All relevant data are within the paper and its Supporting Information files.

References

1. Keall PJ, Mageras GS, Balter JM et al. The management of respiratory motion in radiation oncology report of AAPM Task Group 76. Med. Phys. 2006;33(10):3874-900.
2. Chung H, Cho S, Cho B. Feasibility Study of Robotics-based Patient Immobilization Device for Real-time Motion Compensation. Prog Med Phys. 2016;27(3):117-24.
3. Depuydt T, Verellen D, Haas O et al. Geometric accuracy of a novel gimbals based radiation therapy tumor tracking system. Radiother Oncol. 2011;98(3):365-72.
4. Engelsman M, Sharp GC, Bortfeld T et al. How much margin reduction is possible through gating or breath hold? Phys. Med. Biol. 2005;50(3):477-90.
5. Stevens CW, Munden RF, Forster KM et al. Respiratory-driven lung tumor motion is independent of tumor size, tumor location, and pulmonary function. Int. J. Radiation Oncology Biol. Phys. 2001;51(1):62-8.
6. Sharp GC, Jiang SB, Shimizu S, Shirato H. Prediction of respiratory tumour motion for real-time image-guided radiotherapy. Phys. Med. Biol. 2004;49(3):425-40.
7. Murphy MJ. Tracking moving organs in real time. Semin Radiat Oncol. 2004;14(1):91-100.
8. Putra D, Haas OCL, Mills JA, Burnham KJ. A multiple model approach to respiratory motion prediction for real-time IGRT. Phys. Med. Biol. 2008;53(6):1651-63.
9. Murphy MJ, Pokhrel D. Optimization of an adaptive neural network to predict breathing. Med. Phys. 2009; 36(1):40-7.
10. Kalet A, Sandison G, Wu H, Schmitz R. A state-based probabilistic model for tumor respiratory motion prediction. Phys. Med. Biol. 2010;55(24):7615-31.
11. Ren Q, Nishioka S, Shirato H, Berbeco RI. Adaptive prediction of respiratory motion for motion compensation radiotherapy. Phys. Med. Biol. 2007;52(22):6651-61.

12. Ernst F, Schweikard A. Predicting respiratory motion signals for image-guided radiotherapy using multi-step linear methods (MULIN). Int J Comput Assist Radiol Surg. 2008;3(1):85-90.
13. Ernst F, Schlaefer A, Schweikard A. Prediction of Respiratory Motion with Wavelet-Based Multiscale Autoregression. Proc. of the 10th int. conf. on Medical image computing and computer-assisted intervention, MICCAI (Berlin, Germany) 2007;668-75.
14. Chiesa S, Placidi L, Azario L et al. Adaptive optimization by 6 DOF robotic couch in prostate volumetric IMRT treatment: rototranslational shift and dosimetric consequences. J Appl Clin Med Phys. 2015;16(5):35-45.
15. D'Souza WD, Naqvi SA, Yu CX. Real-time intra-fraction-motion tracking using the treatment couch: a feasibility study. Phys. Med. Biol. 2005;50:4021-33.
16. Kilby W, Dooley JR, Kuduvalli G, et al. The CyberKnife Robotic Radiosurgery System in 2010. Technol. Cancer Res. Treat. 2010;9(5):433-52.
17. Diebel J. Representing Attitude: Euler Angles, Unit Quaternions, and Rotation Vectors. Matrix. 2006;58:1-35.
18. Krilavicius T, Zliobaite I, Simonavicius H, Jarusevicius L. Predicting respiratory motion for real-time tumour tracking in radiotherapy. 2016 IEEE 29th International Symposium on Computer-Based Medical Systems (CBMS), (Dublin, Ireland) 2016;1-33.